Neuron
Article

Anti-Tau Antibodies that Block Tau Aggregate Seeding In Vitro Markedly Decrease Pathology and Improve Cognition In Vivo

Kiran Yanamandra,[1,2,3] Najla Kfoury,[1,2,3] Hong Jiang,[1,2,3] Thomas E. Mahan,[1,2,3] Shengmei Ma,[1,2,3] Susan E. Maloney,[4] David F. Wozniak,[4] Marc I. Diamond,[1,2,3,5,*] and David M. Holtzman[1,2,3,5,*]
[1]Department of Neurology
[2]Hope Center for Neurological Disorders
[3]Charles F. and Joanne Knight Alzheimer's Disease Research Center
[4]Department of Psychiatry
Washington University School of Medicine, St. Louis, MO 63110, USA
[5]These authors contributed equally to this work
*Correspondence: diamondm@neuro.wustl.edu (M.I.D.), holtzman@neuro.wustl.edu (D.M.H.)
http://dx.doi.org/10.1016/j.neuron.2013.07.046

SUMMARY

Tau aggregation occurs in neurodegenerative diseases including Alzheimer's disease and many other disorders collectively termed tauopathies. *trans*-cellular propagation of tau pathology, mediated by extracellular tau aggregates, may underlie pathogenesis of these conditions. P301S tau transgenic mice express mutant human tau protein and develop progressive tau pathology. Using a cell-based biosensor assay, we screened anti-tau monoclonal antibodies for their ability to block seeding activity present in P301S brain lysates. We infused three effective antibodies or controls into the lateral ventricle of P301S mice for 3 months. The antibodies markedly reduced hyperphosphorylated, aggregated, and insoluble tau. They also blocked development of tau seeding activity detected in brain lysates using the biosensor assay, reduced microglial activation, and improved cognitive deficits. These data imply a central role for extracellular tau aggregates in the development of pathology. They also suggest that immunotherapy specifically designed to block *trans*-cellular aggregate propagation will be a productive treatment strategy.

INTRODUCTION

Tau is a microtubule-associated protein that forms intracellular aggregates in several neurodegenerative diseases collectively termed tauopathies. These include Alzheimer's disease (AD), progressive supranuclear palsy (PSP), corticobasal degeneration (CBD), and frontotemporal dementia (FTD) (Mandelkow and Mandelkow, 2012). Tau is a highly soluble and natively unfolded protein (Jeganathan et al., 2008) that binds and promotes the assembly of microtubules (Drechsel et al., 1992; Witman et al., 1976). In tauopathies, tau accumulates in hyperphosphorylated neurofibrillary tangles (NFTs) that are visualized within dystrophic neurites and cell bodies (Mandelkow and Mandelkow, 2012). The amount of tau pathology correlates with progressive neuronal dysfunction, synaptic loss, and functional decline in humans and transgenic mouse models (Arriagada et al., 1992; Bancher et al., 1993; Polydoro et al., 2009; Small and Duff, 2008).

In human tauopathies, pathology progresses from one brain region to another in disease-specific patterns (Braak and Braak, 1997; Raj et al., 2012; Seeley et al., 2009; Zhou et al., 2012), although the underlying mechanism is not yet clear. The prion hypothesis holds that tau aggregates escape cells of origin to enter adjacent cells, where they seed further tau aggregation and propagate pathology (Frost and Diamond, 2010). We have previously observed that recombinant tau fibrils will induce aggregation of full-length intracellular tau in cultured cells and that aggregated forms of tau transfer between cells (Frost et al., 2009). Further, we found that intracellular tau fibrils are released free into the media, where they propagate aggregation by direct interaction with native tau in recipient cells. An anti-tau antibody (HJ9.3) blocks this process by preventing tau aggregate uptake into recipient cells (Kfoury et al., 2012). In addition to similar experiments with recombinant tau (Guo and Lee, 2011), others have shown that paired helical filaments from AD brain induce cytoplasmic tau aggregation (Santa-Maria et al., 2012). Injection of brain extract from human P301S tau transgenic mice into the brains of mice expressing wild-type human tau induces assembly of wild-type human tau into filaments and spreading of pathology (Clavaguera et al., 2009). Similar effects occurred after injection of recombinant full-length or truncated tau fibrils, which caused rapid induction of NFT-like inclusions that propagated from injected sites to connected brain regions in a time-dependent manner (Iba et al., 2013). Selective tau expression in the entorhinal cortex caused late pathology in the axonal terminal zones in cells in the dentate gyrus and hippocampus, consistent with transsynaptic movement of aggregates (de Calignon et al., 2012; Liu et al., 2012). A growing body of work thus supports the idea that tau aggregates transfer between cells and might be targeted with therapeutic antibodies.

In mouse models that mimic aspects of AD and Parkinson's disease, passive immunization using antibodies against Aβ and

alpha synuclein can reduce Aβ and alpha-synuclein deposition in brain (Bard et al., 2000; DeMattos et al., 2001; Masliah et al., 2011) and improve behavioral deficits (Dodart et al., 2002; Kotilinek et al., 2002; Masliah et al., 2011). Active immunization in tauopathy mouse models using tau phospho peptides reduced tau pathology (Bi et al., 2011; Boimel et al., 2010) and in some studies improved behavioral deficits (Asuni et al., 2007; Boutajangout et al., 2010; Troquier et al., 2012). In two passive vaccination studies, there was reduced tau pathology and improved motor function when the antibody was given prior to the onset of pathology (Boutajangout et al., 2011; Chai et al., 2011). While several of the tau immunization studies appear to show some beneficial effects, the maximal expected efficacy of anti-tau antibodies administered after the onset of pathology, the optimal tau species to target, and the mechanism of the therapeutic effect have remained unknown.

Our prior work in cell culture has suggested that aggregate flux in and out of cells might be central to progressive pathology (Kfoury et al., 2012). Thus, we predicted that antibodies that specifically block P301S brain-derived seeding activity might block propagation between cells and decrease overall tau pathology. We have used P301S human tau transgenic mice (Yoshiyama et al., 2007) to test intracerebroventricular (ICV) administration of three different anti-tau antibodies selected for their ability to block tau seeding activity in vitro and to block tau uptake into cells.

RESULTS

Characterization of Anti-Tau Antibodies

We have previously observed that tau aggregates, but not monomer, are up taken by cultured cells and that internalized tau aggregates trigger intracellular tau aggregation in recipient cells (Frost et al., 2009; Kfoury et al., 2012). We characterized the HJ8 series of eight mouse monoclonal antibodies (raised against full-length human tau) and HJ9 series of five antibodies (raised against full-length mouse tau) in an adapted cellular biosensor system we have previously described (Kfoury et al., 2012) that measures cellular tau aggregation induced by the addition of brain lysates containing tau aggregates. The antibodies had variable effects in blocking seeding, despite the fact that all antibodies efficiently bind tau monomer and stain neurofibrillary tangles. We selected three antibodies with different potencies in blocking seeding for our studies.

Prior to testing in vivo, we determined the binding affinities and epitopes of the antibodies, which are all IgG2b isotype. We immobilized human and mouse tau on a sensor chip CM5 for surface plasmon resonance (SPR) (Figure 1). The HJ9.3 antibody, raised against mouse tau, recognizes both human (Figure 1A) and mouse (Figure 1B) tau with the same binding constant ($K_D = K_d/K_a$ = 100 pM) (Figure 1G). The association (K_a) and dissociation (K_d) rate constants were calculated by using BIAevaluation software (Biacore AB) selecting *Fit kinetics simultaneous* K_a/K_d (Global fitting) with 1:1 (Langmuir) interaction model. The K_a and K_d of HJ9.3 toward human (K_a = 7.5 × 10^4 Ms^{-1}, K_d = 7.5 × 10^{-6} s^{-1}) and mouse (K_a = 8.6 × 10^4 Ms^{-1}, K_d = 9.1 × 10^{-6} s^{-1}) indicate strong binding to both. We mapped the epitope of HJ9.3 to the repeat domain (RD) region, between amino acids 306–320. HJ9.4, raised against mouse tau, had high affinity K_D (2.2 pM) toward mouse tau with a high association rate constant (K_a = 2.28 × 10^5 Ms^{-1}) and very low dissociation constant (K_d = 5.1 × 10^{-7} s^{-1}) (Figures 1D and 1G). However, the same antibody had a much lower affinity (K_D = 6.9 nM) toward human tau (Figures 1C and 1G), with a similar association rate constant (K_a = 1.5 × 10^5 Ms^{-1}) as mouse tau but with much faster dissociation (K_d = 1.07 × 10^{-3} s^{-1}). Thus, the HJ9.4 interaction with human tau is less stable than with mouse tau. The epitope for this antibody is amino acids 7–13. HJ8.5 was raised against human tau. It binds to human tau (Figure 1E) but not to mouse tau (Figure 1F). The K_D (0.3 pM) (Figures 1E and 1G) and low dissociation rate (K_d = 4.38 × 10^{-8} s^{-1}) indicate that HJ8.5 binds human tau with very high affinity. We mapped the epitope of HJ8.5 to amino acids 25–30. All three anti-tau antibodies strongly recognized human tau fibrils on SPR (Figure S1 available online). Because the fibrils have multiple identical epitopes, we could not directly calculate the association and dissociation rates.

We also assessed the antibodies by immunoblotting and immunostaining. On western blots, all three antibodies bound to human tau (Figure 1H). HJ9.3 and HJ9.4 bound to mouse tau, while HJ8.5 did not (Figure 1H). Consistent with our prior findings (Yamada et al., 2011), there appeared to be less reassembly buffer (RAB)-soluble tau in 9-month-old compared to 3-month-old P301S mice. We found that HJ8.5 stained human tau in 3-month-old and 9- to 12-month-old transgenic P301S mouse brains. Tau immunoreactivity was present throughout the cell bodies and processes (Figure S2). In 9- to 12-month-old P301S mice with tau aggregates, HJ8.5 detected tau aggregates in cell bodies (Figure S2A). Other antibodies produced similar results (Figure S2B). All antibodies bound to neurofibrillary tangles and neuropil threads in AD brain (Figure S2).

Tau Antibodies Block the Uptake and Seeding Activity of P301S Tau Aggregates

To evaluate seeding activity present in P301S brain lysates, we adapted a cellular biosensor system that we have previously described (Kfoury et al., 2012). This is based on expression of the repeat domain of tau (aa 243–375) containing the ΔK280 mutation fused either to cyan or yellow fluorescent protein (RD(ΔK)-CFP/YFP). Uptake of exogenous aggregates into these cells triggers intracellular aggregation of RD(ΔK)-CFP/YFP that is detected by fluorescence resonance energy transfer (FRET) recorded on a fluorescence plate reader (Kfoury et al., 2012). Clarified brain lysates from 12-month-old P301S mice added to the biosensor cell system induced strong aggregation of the RD(ΔK)-CFP/YFP reporter, indicating the presence of tau seeding activity (Figure 2A). The seeding activity from 12-month-old P301S brain homogenate mice roughly corresponds to 50 nM (monomer equivalent) of recombinant full-length fibrils (data not shown).

There was little to no aggregation induced by lysates from tau knockout mice, wild-type mice, or 3-month-old P301S mice lacking tau pathology (Figure 2A). We assessed the anti-tau antibodies (HJ8.5, HJ9.3, and HJ9.4) for their ability to block the uptake and seeding activity from the 12-month-old P301S brain lysates. HJ3.4 (mouse monoclonal anti-Aβ antibody) was

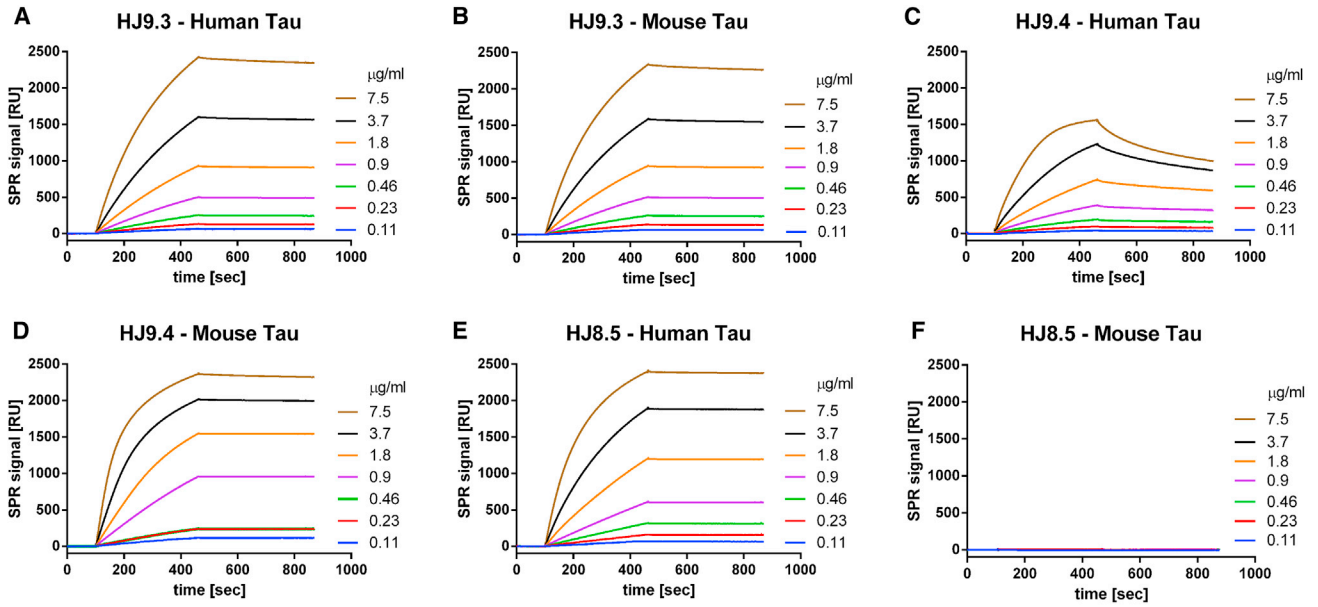

G

		HJ9.3	HJ9.4	HJ8.5
Humuan tau	K_a (Ms^{-1})	7.55 x 10^4	1.53 x 10^5	1.3 x 10^5
	K_d (s^{-1})	7.51 x 10^{-6}	1.07 x 10^{-3}	4.34 x 10^{-8}
	K_D (M)	99 pM	6.9 nM	0.336 pM
Mouse tau	K_a (Ms^{-1})	8.61 x 10^4	2.28 x 10^5	-
	K_d (s^{-1})	9.16 x 10^{-6}	5.1 x 10^{-7}	-
	K_D (M)	100 pM	2.24 pM	-

H

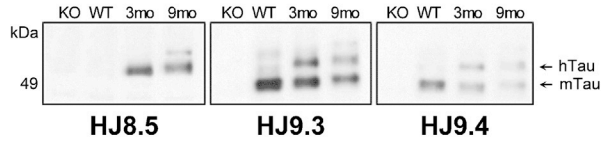

Figure 1. Characterization of Anti-Tau Antibodies by Surface Plasmon Resonance and Immunoblotting

Surface plasmon resonance (SPR) sensorgrams showing the binding of each anti-tau antibody toward immobilized recombinant human tau (longest isoforms hTau40, 441 aa) and immobilized mouse tau (longest isoforms mTau40, 432 aa). Each antibody was run with various concentrations (0.11, 0.23, 0.46, 0.90, 1.8, 3.7, and 7.5 µg/ml) and plots are shown in the corresponding color.

(A and B) SPR sensorgrams of HJ9.3 antibody binding to immobilized human tau (A) and immobilized mouse tau (B).

(C and D) SPR sensorgrams of HJ9.4 antibody binding to immobilized human tau (C) and immobilized mouse tau (D).

(E and F) SPR sensorgrams of HJ8.5 antibody binding to immobilized human tau (E) and mouse tau (F).

(G) Table showing the association rate constant (K_a), dissociation rate constant (K_d), and binding constant (K_D) of each antibody toward human and mouse tau. BIAevaluation software (Biacore AB) was used to calculate K_a and K_d by selecting *Fit kinetics simultaneous K_a/K_d* (Global fitting) with 1:1 (Langmuir) interaction model. Ms^{-1}, millisecond; M, molar; s, second.

(H) RAB-soluble fractions of 3-month-old tau knockout (KO), 3-month-old wild-type (WT), 3-month-old P301S (3mo), and 9-month-old P301S (9mo) mice were analyzed by immunoblot by using the indicated anti-tau antibodies.

a negative control. The anti-tau antibodies effectively blocked seeding activity (Figure 2B). To determine their relative efficacy, we titrated the antibodies (0.125, 0.25, 0.5, 1, and 2 µg/ml) against a fixed amount of P301S brain lysate (Figure 2C). The HJ8.5 antibody blocked seeding activity at concentrations as low as 0.25 µg/ml compared to controls. At 0.5 µg/ml, both HJ8.5 and HJ9.3 antibody significantly blocked uptake and seeding activity compared to control. HJ9.4 was least potent in blocking the uptake and seeding activity, consistent with its higher affinity for mouse tau. All three anti-tau antibodies detected tau aggregates internalized after uptake by HEK293 cells, as detected by post hoc cellular permeabilization and staining. However, when these antibodies were preincubated with and without P301S brain lysates, none of these antibodies were detected inside cells upon staining with anti-mouse secondary antibody (Figure S3). While other modes of inhibition are possible, these data are consistent with a mechanism based on blocking cellular uptake of tau aggregates.

To further assess tau seeding activity present in TBS-soluble P301S brain lysates, we immunoprecipitated lysates with the different antibodies and assessed both the bound and unbound fractions for seeding activity. After control HJ3.4 immunoprecipitation, the unbound fraction had strong seeding activity and the immunoprecipitated material had no seeding activity (Figure 2D). After immunoprecipitaton with HJ8.5 and HJ9.3, the unbound fraction had no significant seeding activity, and with HJ9.4, the

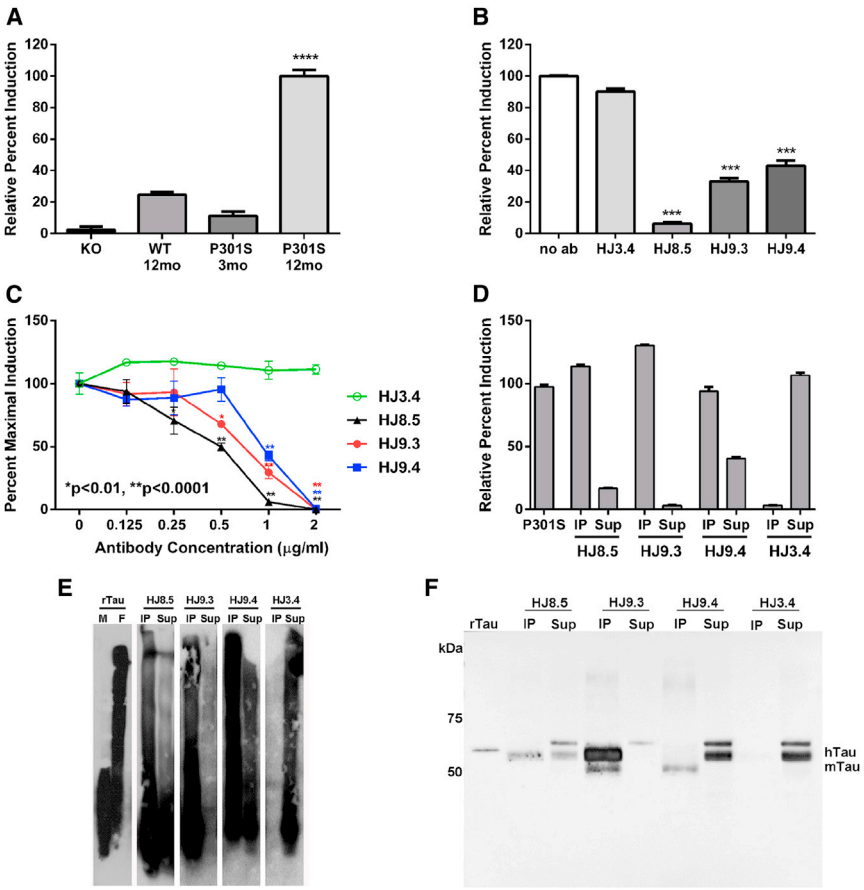

Figure 2. Tau Antibodies Block the Uptake and Seeding Activity of P301S Tau Aggregates as Detected by a FRET Assay

(A) HEK293 cells expressing RD (ΔK280)-CFP/YFP were exposed to 2.5 μg of total protein of 1 × TBS brain lysates for 24 hr. Brain lysates collected from 12-month-old P301S mice induced much greater seeding activity (n = 5) as compared to lysates from knockout (KO) mice (n = 7), wild-type (WT) mice (n = 6), or young 3-month-old P301S mice (n = 2). ****p < 0.0001 versus other groups.

(B) HEK293 cells were cotransfected with RD (ΔK280)-CFP and RD (ΔK280)-YFP. Eighteen hours later, preincubated P301S brain lysates with or without incubation of anti-tau antibodies (HJ8.5, HJ9.3, and HJ9.4) or control antibody (HJ3.4, anti Aβ antibody) were added to cells. We found all the tau antibodies incubated with P301S brain lysates significantly blocked seeding activity. Statistical significance was determined by one-way ANOVA followed by Dunnett's post hoc test for multiple comparisons by using GraphPad Prism 5.0 software. ***p > 0.001.

(C) Titration of these antibodies with various concentrations (0.125 μg/ml, 0.25 μg/ml, 0.5 μg/ml, 1 μg/ml, and 2 μg/ml) was performed with a fixed amount of P301S brain lysates. Twenty-four hours later, FRET analysis was performed. Out of all tau antibodies we used, HJ8.5 was the most potent in blocking the uptake and seeding activity of P301S brain lysates. Statistical significance was determined by two-way ANOVA followed by Bonferroni post hoc test for multiple comparisons. **p < 0.0001, *p < 0.01. Values represent mean ± SEM.

(D–F) Immunoprecipitated (IP) and depleted supernatant (Sup) of P301S brain lysate of all anti-tau antibodies (HJ8.5, HJ9.3, and HJ9.4) and control antibody (HJ3.4) were analyzed by tau seeding assay (D), SDD-AGE followed by western blot (E), and SDS-PAGE followed by western blot (F). Monomeric (M) and fibrillized (F) recombinant human tau (rTau) was used as controls for SDD-AGE and monomeric rTau was used for SDS-PAGE as a control. hTau indicates human tau and mTau indicates endogenous mouse tau.

unbound material had reduced seeding activity. After elution from the anti-tau antibodies, the immunoprecipitated material had strong seeding activity. To assess the tau seeds, we analyzed these fractions by nondenaturing blots (semidenaturing detergent-agarose gel electrophoresis [SDD-AGE]) (Halfmann and Lindquist, 2008) and by denaturing blots (SDS-PAGE) followed by western blotting for tau. SDD-AGE of immunoprecipitated tau revealed monomer and multiple larger species that are probably oligomeric (Figure 2E). The unbound material had some residual tau species but less than what was present in the immunoprecipated material. HJ3.4 did not immunoprecipitate any tau species. Western blot following SDS-PAGE (Figure 2F) revealed that the tau multimers were denatured to predominantly tau monomer, but the overall patterns were similar. Although tauopathy is associated with detergent-insoluble tau, we observed that TBS-soluble brain lysates contain tau seeding activity. To characterize the tau present in this fraction, we evaluated the immunoprecipitated material by atomic force microscopy (AFM). HJ3.4 immunoprecipiated no aggregated material. Interestingly, each tau antibody immunoprecipitated unique forms of aggregated material (Figure 3), consistent with a multiplicity of aggregated tau species.

Intracerebroventricular Infusion of Anti-Tau Antibodies

In our colonies, P301S mice first develop intracellular tau pathology beginning at 5 months of age. To test the efficacy of the three antibodies by chronic intracerebroventricular (ICV) administration, we surgically implanted a catheter into the left lateral ventricle of each mouse at 6 months of age and continuously infused anti-tau antibodies for 3 months via Alzet subcutaneous osmotic minipump (Figure S4A). We used anti-Aβ antibody HJ3.4 and PBS as negative controls. After 6 weeks, we replaced each pump with one filled with fresh antibody solution or PBS. At the time of brain dissection, we verified catheter placement in the left lateral ventricle of each mouse by cresyl violet staining (Figure S4B). Only mice with correctly placed catheters were included in the analyses. To test the stability of the antibodies after 6 weeks in vivo (Figure S4A), we collected residual pump contents upon removal from the animals and assessed the antibodies using SDS-PAGE and Coomassie blue staining. Light and heavy chains were intact, with no fragmentation, and retained tau binding activity on western blot (data not shown). To estimate the concentration of anti-tau antibodies in CSF and serum during the infusion, we administered biotinylated HJ8.5 (HJ8.5B) for 48 hr (~7.2 μg/day) (Figure S4A). The concentration of free

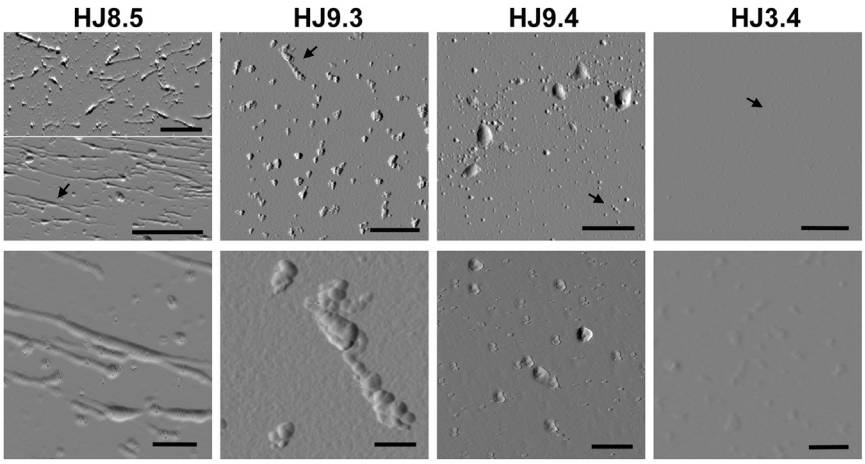

Figure 3. AFM Analysis of Isolated Tau Aggregates from P301S Mouse Brain

Tau aggregates were isolated by IP from TBS lysates of 12-month-old P301S mouse brains by using anti-tau antibodies (HJ8.5, HJ9.3, and HJ9.4) and control antibody HJ3.4. Each column represents the IP material from each antibody. Black arrows indicate the areas magnified. Bottom panel shows a magnified area of the top panel. Scale bar represents 1 μm in all top panel images and represents 200 nm in bottom panel images. Morphology of the aggregated species IPed by each anti-tau antibody appears unique. Anti-Aβ antibody HJ3.4 did not IP any aggregates.

HJ8.5B was 7.3 μg/ml in the CSF and 6.2 μg/ml in the serum, indicating clearance of the antibody from the CNS to the periphery (Figure S4C). We also detected HJ8.5B bound to human tau in both CSF and serum, though the concentration was lower than that of free antibody (Figure S4C).

Anti-Tau Antibody Treatment Reduces Abnormally Phosphorylated Tau

To determine the extent of tau pathology in P301S mice after 3 months of treatment, we carried out multiple stains for tau pathology. Brain sections were first assessed by immunostaining with the anti-phospho tau antibody AT8 (Figure 4). AT8 binds phosphorylated residues Ser^{202} and Thr^{205} of both mouse and human tau (Figure 4) (Goedert et al., 1995). In mice treated with PBS and HJ3.4, AT8 strongly stained neuronal cell bodies and the neuropil in multiple brain regions, particularly in the piriform cortex, entorhinal cortex, amygdala, and hippocampus (Figures 4A and 4B). HJ8.5 treatment strongly reduced AT8 staining (Figure 4C), especially in the neuropil. HJ9.3 and HJ9.4 also decreased AT8 staining but the effects were slightly less (Figures 4D and 4E). Quantitative analysis of AT8 staining in piriform cortex (Figure 5A), entorhinal cortex (Figure 5B), and amygdala (Figure 5C) demonstrated a strong but variable reduction in phospho-tau in all anti-tau antibody-treated mice. HJ8.5 antibody markedly reduced AT8 staining in piriform cortex, entorhinal cortex, and amygdala. HJ9.3 had slightly decreased effects compared to HJ8.5, and HJ9.4 had significant effects in both entorhinal cortex and amygdala but not in the piriform cortex (Figure 5). The hippocampus exhibited much more variable AT8 staining versus other brain regions, predominantly in cell bodies, and thus was not statistically different in treatment versus control groups (Figure 5D). Because it has been reported that male P301S mice have greater tau pathology than females (Zhang et al., 2012), we also assessed the effect of both gender and treatment (Figure S5). In addition to an effect of treatment, there was significantly more AT8 staining in all brain regions analyzed in male mice (Figure S5C). However, the effects of the antibodies were still highly significant and virtually identical after adjusting for gender (Figure S5D). We also compared the treatment groups versus controls in males and females separately, and the effects of antibody HJ8.5 remained most significant (Figures S5A and S5B).

Correlation of Multiple Staining Modalities

To test for tau amyloid deposition, we used thioflavin S (ThioS) to stain brain sections (Figure S6). We semiquantitatively assessed ThioS staining using a blinded rater who gave a score from 1 (no staining) to 5 (maximum staining) in all control and anti-tau antibody-treated mice. By semiquantitative assessment, HJ8.5 treatment significantly reduced ThioS staining compared to PBS and HJ3.4 (Figures 6A and 6B). We also stained mice treated with PBS, HJ8.5, and HJ9.3 ($n = 6$ from each group) with PHF1 monoclonal antibody, which recognizes tau phospho-residues Ser^{396} and Ser^{404} (Otvos et al., 1994). AT8 and PHF1 staining significantly correlated ($r = 0.630$, $p = 0.005$) (Figure S7A), showing that two anti-phospho tau antibodies to different tau epitopes give similar results.

Many neurodegenerative diseases, including tauopathies, exhibit microglial activation in areas of the brain surrounding protein aggregation and cell injury. We assessed microglial activation in the treatment groups using anti-CD68 antibody (Macauley et al., 2011) (Figures S6C–S6G). HJ8.5 and HJ9.3 treatment reduced microglial activation in piriform cortex, entorhinal cortex, and amygdala compared to controls (Figures S6C–S6G). HJ9.4 had a weaker effect in the piriform cortex compared to HJ8.5 and HJ9.3 (Figures S6E–S6G), consistent with the AT8 staining results (Figure 4A). Microglial activation strongly correlated with AT8 staining in all samples ($r = 0.511$, $p = 0.0038$) (Figure S7B).

Anti-Tau Antibodies Reduce Detergent-Insoluble Tau and Seeding Activity

To determine the level of soluble and insoluble tau in the cortex, we performed sequential biochemical extraction with RAB (aqueous buffer), radio immunoprecipitation assay (RIPA) (detergent buffer), and 70% formic acid (FA) to solubilize the final pellet. We quantified total tau by ELISA with anti-tau antibody HJ8.7, which detects both human and mouse tau with the same K_D (0.34 pM). We excluded the possibility that the treatment antibodies would interfere with the ELISA by spiking

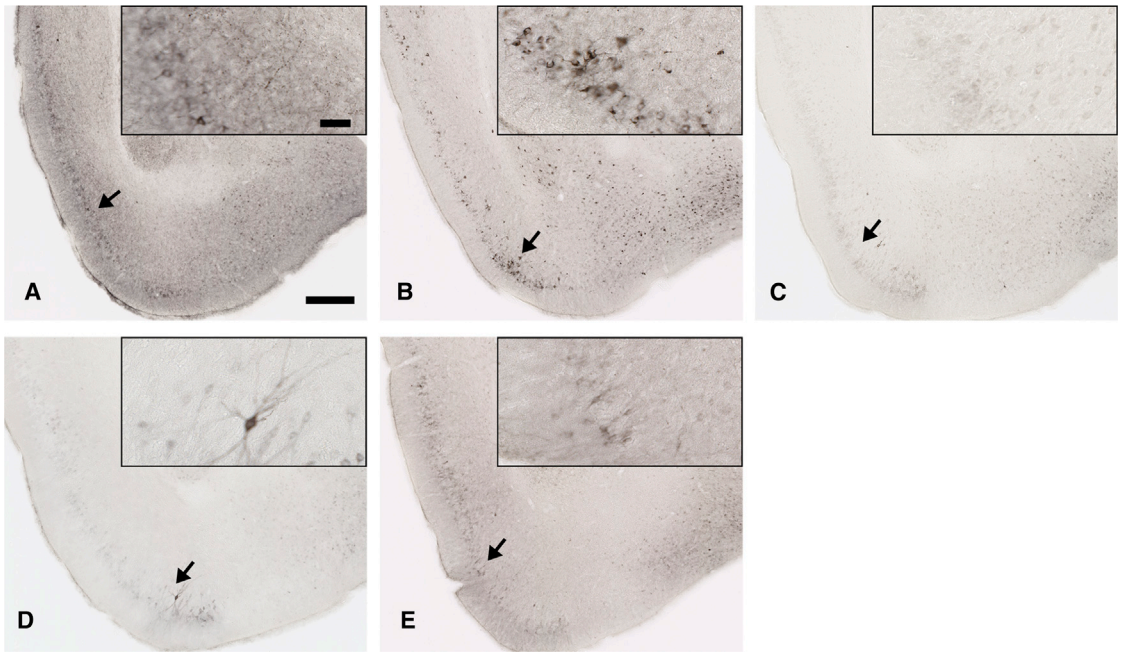

Figure 4. Anti-Tau Antibodies Strongly Decreased AT8 Staining in P301S Mouse Brain

Representative coronal sections of PBS (A)-, HJ3.4 antibody (B)-, HJ8.5 antibody (C)-, HJ9.3 antibody (D)-, and HJ9.4 antibody (E)-treated 9-month-old P301S mice stained with biotinylated AT8 antibody in regions including the piriform cortex and amygdala. Scale bar represents 250 μm. Insets in (A)–(E) show the higher magnification of biotinylated AT8 antibody staining of phosphorylated tau, scale bar represents 50 μm.

positive control samples with these antibodies prior to analysis and observing no interference (data not shown). We analyzed all mice that were assessed by pathological analysis in Figure 5. Total tau levels in the RAB (Figure 6A)- or RIPA (Figure 6B)-soluble fractions were similar among all groups. We analyzed the detergent-insoluble/70% FA-soluble fractions by neutralizing the samples prior to ELISA and western blot. We analyzed every animal studied and found that HJ8.5 and HJ9.3 decreased detergent-insoluble tau by >50% versus controls (Figure 6C). Representative samples (n = 4 from each group) illustrate by western blot decreased levels of insoluble tau in mice treated with HJ8.5 and HJ9.3 (Figure S7C). Insoluble tau levels were no different in HJ9.4-treated groups versus PBS or HJ3.4. We also assessed human and mouse tau specifically in the detergent-insoluble/70% FA-soluble fractions in n = 6 mice per group in which the mean AT8 staining reflected the mean values of results in Figure 4. There was significantly more human tau than mouse tau in the 70% FA-soluble fraction, and the antibodies significantly lowered human but not mouse tau in this fraction (Figures 6D and 6E). In these same samples, we assessed levels of AT8 immunoreactive signal by ELISA. The AT8 signal was lower in the antibody-treated samples (Figure 6F), similar to what was seen for total tau in this fraction.

We hypothesized that a reduction of tau aggregation in brain would correlate with a reduction in seeding activity. Thus, we used the cellular biosensor assay to test for P301S brain seeding activity in the cortical RAB-soluble fractions from the different treatment groups. Our prior data assessing ISF tau in P301S mice suggested the possible presence of extracellular tau aggregates in equilibrium with both the biochemically soluble and insoluble pools of tau (Yamada et al., 2011). We first assessed intracellular aggregation of RD(ΔK)-CFP/YFP after treating the cells with lysates from mice treated with PBS or HJ3.4. Lysates from these groups strongly induced FRET signal (Figure 7A). We observed markedly less seeding activity in lysates from the cortical tissue of mice treated with HJ8.5 and HJ9.3 (Figure 7A). This was not due to residual antibody in the brain lysates, because immunoprecipitation of the brain lysates followed by elution of seeding activity from the antibody/bead complexes produced the same pattern (Figure 7B). Thus, HJ8.5 and HJ9.3 reduce seeding activity in the P301S tau transgenic mouse brain. HJ9.4 did not significantly reduce seeding activity (Figure 7A). Seeding activity strongly correlated with the amount of detergent-insoluble/formic acid-soluble tau detected by ELISA (Pearson's r = 0.529, p = 0.0001) (Figure 7C) but did not correlate with total tau in RAB fractions (Figure 7D). We hypothesized that seeding activity is due to tau aggregates present in the RAB-soluble fraction. To test for this, we performed SDD-AGE followed by western blot. In addition to tau monomer, we observed higher molecular weight tau species present in 3-month-old P301S mice and a larger amount present in 9-month-old P301S mice (Figure 7E). A component of these higher molecular weight species probably constitutes the seeding activity detected in the FRET assay and may be in equilibrium with the tau present in the detergent-insoluble/formic acid-soluble fraction.

Anti-Tau Antibodies Rescue Contextual Fear Deficits

In studies of P301S tau transgenic mice at 9 months of age, we compared the control and anti-tau antibody-treated groups in a variety of behaviors. The groups did not differ in locomotor

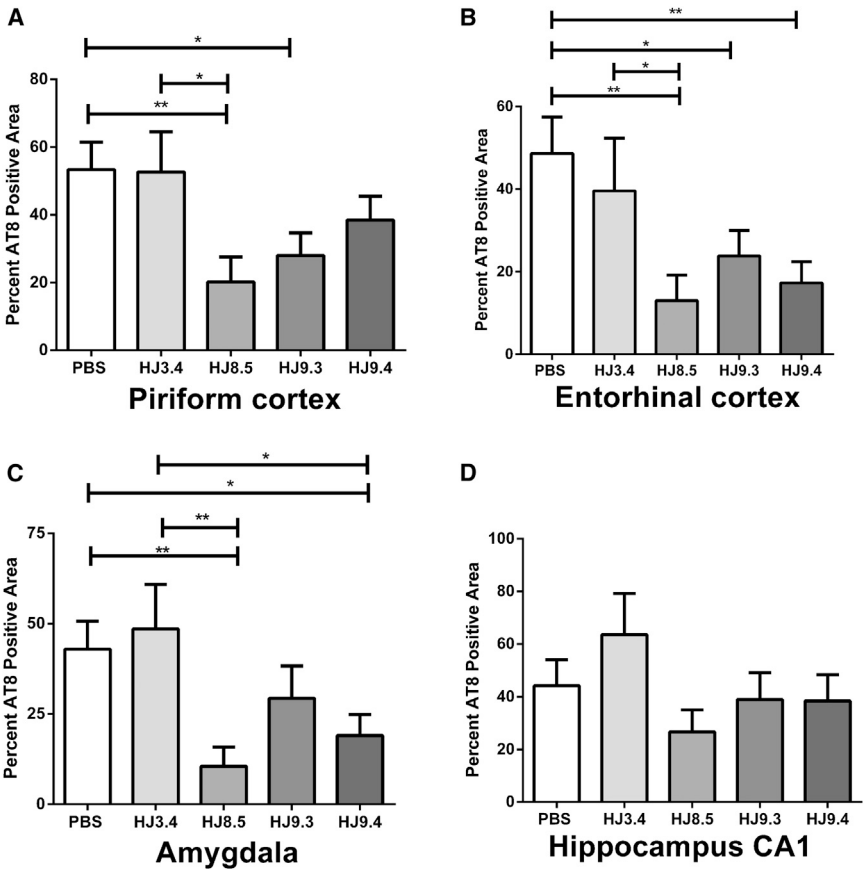

Figure 5. Certain Anti-Tau Antibodies Strongly Decrease AT8 Staining in P301S Mouse Brain

Percent of the area covered by biotinylated AT8 staining of abnormally phosphorylated tau in piriform cortex (A), entorhinal cortex (B), amygdala (C), and hippocampus CA1 region (D) in mice treated with the anti-tau antibodies HJ8.5 (n = 13), HJ9.3 (n = 15), HJ9.4 (n= 13), the anti-Aβ antibody, HJ3.4 (n = 8), or PBS (n = 16) in 9-month-old P301S mice. There was reduced AT8 staining in several different brain regions in the anti-tau antibody-treated mice compared to PBS or HJ3.4 antibody-treated mice. HJ8.5 had the largest effects. $^{**}p < 0.01$, $^{*}p < 0.05$, values represent mean ± SEM.

activity, exploration, or measures of sensorimotor function (Figure S8). The ability of the anti-tau antibody treatments to rescue cognitive deficits in P301S mice was evaluated by assessing the performance of the mice on the conditioned fear procedure. On day 1, all four treatment groups of mice exhibited similar levels of baseline freezing during the first 2 min in the training chamber. This was confirmed by repeated-measures ANOVA, which failed to reveal any significant overall main effects or interactions involving treatment (Figure 8A). In addition, all four groups showed similar levels of freezing during the tone-shock (T/S) conditioned stimulus-unconditioned stimulus (CS-US) pairings (Figure 8A). The general lack of differences in freezing levels between groups across the three T/S pairings was documented by a nonsignificant effect of treatment and a nonsignificant genotype by minute interaction.

In contrast to the absence of differences among groups during testing on day 1, there were robust differences in freezing levels from the contextual fear test (form of associative learning) conducted on day 2 between two of the anti-tau antibody groups and the PBS+HJ3.4 control mice (Figure 8B). Subsequent planned comparisons indicated that the HJ8.5 mice showed significantly elevated freezing levels averaged across the 8 min test session (Figure 8C) compared to the PBS+HJ3.4 control group, ($F(1,45) = 8.30$, $p = 0.006$), as did to a lesser extent the HJ9.4 mice, ($F(1,45) = 5.60$, $p = 0.022$). Thus, HJ8.5 appeared to have a stronger effect overall in preserving associative learning.

DISCUSSION

One model for the pathogenesis of the tauopathies holds that aggregates produced in one cell escape or are released into the extracellular space to promote aggregation in neighboring or connected cells (Clavaguera et al., 2009; de Calignon et al., 2012; Frost et al., 2009; Kfoury et al., 2012; Kim et al., 2010; Liu et al., 2012). We have observed that selection of therapeutic antibodies that specifically block tau seeding activity from brain lysates predicts potent in vivo responses at least as strong if not stronger than prior reports of active or passive tau vaccination. We began with a cellular biosensor assay that is sensitive to the presence of extracellular tau aggregates. We found that brain lysates from P301S transgenic mice contained seeding activity that could induce further intracellular aggregation. After screening a panel of anti-tau antibodies, we selected three with variable activities in blocking tau seeding activity. We infused these antibodies ICV over 3 months into P301S tauopathy mice, beginning at a time when pathology had initiated (6 months). Infusion of the antibodies resulted in appreciable concentrations of antibody present in both CSF and serum, consistent with previous reports of efflux of antibodies from the CNS to the periphery (DeMattos et al., 2001; Strazielle and Ghersi-Egea, 2013). Treatment with HJ8.5, the most potent antibody in vitro, profoundly reduced tau pathology. We detected this effect with multiple independent stains, biochemical analyses of insoluble tau, and by analysis of residual tau seeding activity present in brain lysates. There was also improvement in the one behavioral deficit that we detected in this model. All antibodies block tau aggregate uptake into cells, and none is observed within cells in the presence or absence of extracellular aggregates in our assays. The efficacy of these antibodies implies a clear role for extracellular tau in the pathogenesis of neuropathology that was previously thought to be cell autonomous. This work extends our prior findings, which suggest that aggregate flux may occur in the setting of intracellular pathology, raising the possibility of therapies that can assist

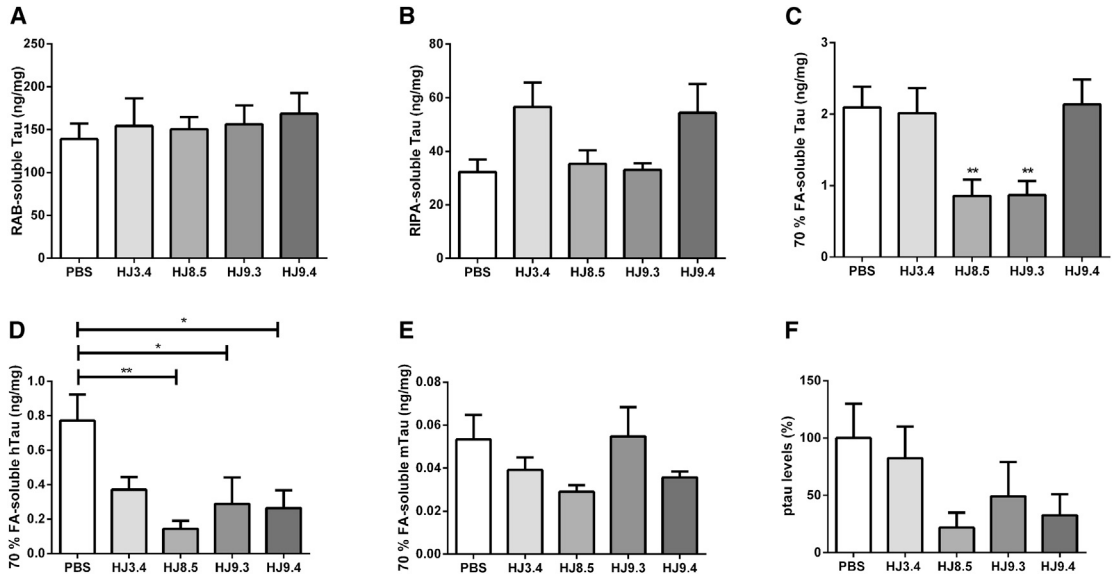

Figure 6. Insoluble Tau Levels Are Reduced by Antibodies HJ8.5 and HJ9.3 in P301S Mice

(A–C) The cortex of all the treated mice (PBS [n = 16], HJ3.4 antibody [n = 8], HJ8.5 [n = 13], HJ9.3 [n = 15], and HJ9.4 [n = 13]) were sequentially extracted by RAB (A), RIPA (B), and 70% FA (C) and their tau levels were quantified by ELISA. There were no statistical differences in soluble tau levels in RAB and RIPA fractions between the groups. However, there was a significant decrease of insoluble tau levels in 70% FA fractions in the HJ8.5 and HJ9.3 anti-tau antibody-treated mice compared to the PBS or HJ3.4 antibody-treated groups. Insoluble tau levels in the HJ9.4 antibody-treated mice were not different from the control groups. $^{**}p < 0.01$.

(D–F) Levels of human tau (D), mouse tau (E), and phospho tau at Ser^{202} and Thr^{205} (F) levels were assessed in 70% FA fractions by specific anti-human, anti-mouse, or anti-phospho tau antibodies by ELISA (n = 6 mice per treatment group). There was a decrease in human tau levels in all groups of anti-tau antibody-treated mice and no change in mouse tau levels. In 70% FA fractions, we also found that phospho tau at Ser^{202} and Thr^{205} as detected by AT8 reactivity was reduced in anti-tau antibody-treated mice compared to controls, similar to total human tau. Values represent mean ± SEM.

in aggregate clearance by targeting extracellular species. This work has important implications for the design of therapeutic antibodies and suggests that targeting seeding activity in particular may produce the most effective agents.

Mechanism-Based Antibody Therapy

Several prior active and passive peripheral immunotherapy approaches against tau have also reduced tau pathology and improved behavioral deficits, but the underlying rationale for antibody choice was based either on a phospho-epitope, reactivity with neurofibrillary tangles, or was not stated (Asuni et al., 2007; Bi et al., 2011; Boimel et al., 2010; Boutajangout et al., 2010, 2011; Chai et al., 2011; Troquier et al., 2012). One tau immunization study, performed by vaccinating mice with full-length tau, induced pathology in wild-type mice (Rosenmann et al., 2006). However, subsequent active immunization approaches with phospho-tau peptides in tau transgenic models reduced tau pathology (Bi et al., 2011; Boimel et al., 2010) and showed behavioral improvement (Asuni et al., 2007; Boutajangout et al., 2010; Troquier et al., 2012). In a passive immunization study, JNPL3 tau transgenic mice were administered the PHF1 antibody intraperitoneally at 2–3 months of age, prior to the onset of tauopathy. PHF-1 targets a pathological form of abnormally phosphorylated tau (Otvos et al., 1994). Treatment reduced tau pathology and improved behavior (Boutajangout et al., 2011). However, while it decreased insoluble phosphorylated tau, total insoluble tau did not change. In another passive immunization study, JNPL3 and P301S mice (at age 2–3 months, prior to the onset of tauopathy) were peripherally administered the PHF1 or MC1 antibody, which targets an aggregate-associated epitope (Jicha et al., 1999). Both treatments improved tau pathology and delayed the onset of motor dysfunction (Chai et al., 2011). In these prior studies, the mechanism of action of the antibodies was not clear, and none was explicitly tested. Indeed, some proposed an intracellular mechanism (Sigurdsson, 2009). Moreover, no study appears to have produced the magnitude of reduction in tau pathology that we observed here, with the caveats that we infused antibodies into the CNS, while the other studies utilized peripheral infusion and different animal models were utilized.

We designed this study explicitly to test a prediction that extracellular tau seeds are a key component of pathogenesis. We began with a selection process to pick antibodies capable of blocking tau seeding in vitro, purposely testing agents with a range of predicted activities. All antibodies that we tested in vivo effectively block aggregate uptake and seeding, providing a basis for their observed activity. We have only tested three therapeutic antibodies in vivo. Thus, the correlations with the in vitro assays could be through chance. Further studies of anti-tau antibodies with variable potencies in the seeding assay will help address this question. In addition, correlation of antibody affinity, epitope, isotype, glycosylation, and ability to bind phosphorylated forms of tau will be important to assess in future studies. This study also reports the effects of direct, intra-CNS infusion of anti-tau antibodies. Despite the fact that the antibodies utilized each target different tau epitopes and do not

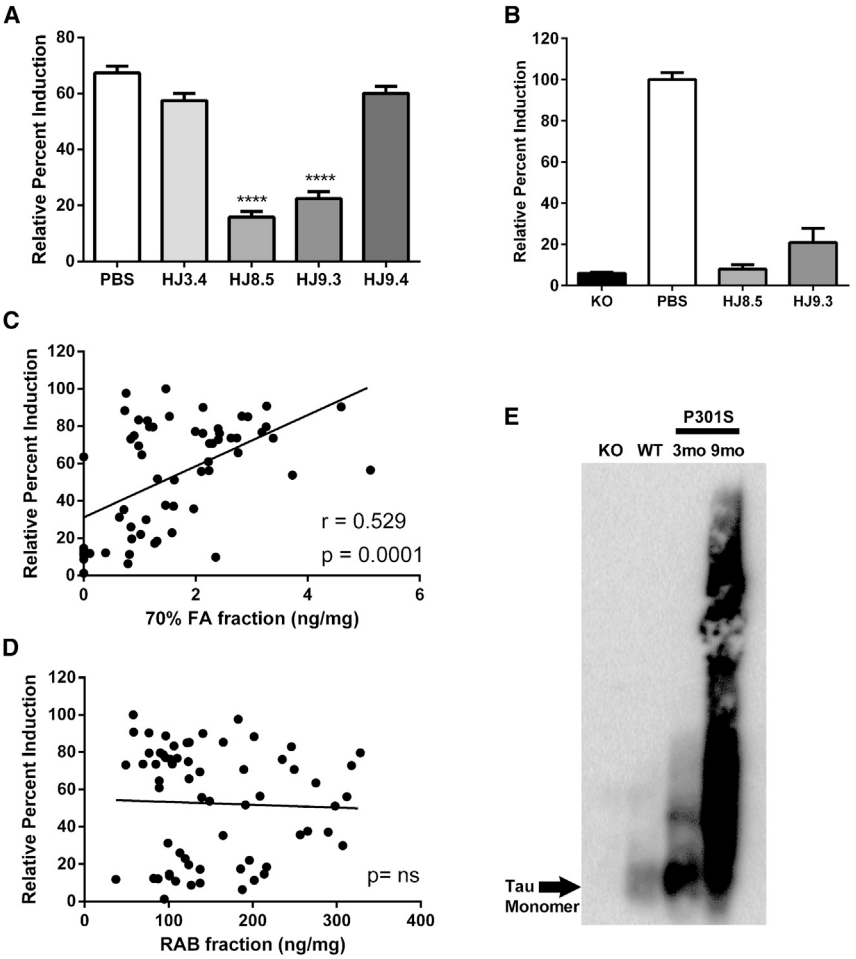

Figure 7. Anti-Tau Antibody-Treated P301S Mice Have Decreased Tau Seeding Activity in Cortical Extracts as Detected by FRET Assay

(A) Tau seeding activity was measured with RAB-soluble fractions of all PBS (n = 16)-, HJ3.4 (n = 8)-, HJ8.5 (n = 13)-, HJ9.3 (n = 15)-, and HJ9.4 (n = 13)-treated mice on HEK293 cells by FRET assay. HEK293 cells were cotransfected with RD (ΔK280)-CFP and RD (ΔK280)-YFP. Eighteen hours later, RAB-soluble fractions were added to cells. Seeding activity was significantly reduced in HJ8.5, and HJ9.3 antibody-treated mice compared to the PBS- or HJ3.4 antibody-treated mice. RAB-soluble fractions from HJ9.4 antibody-treated mice did not have decreased seeding activity compared to the PBS or HJ3.4 antibody RAB-soluble fractions. ***$p < 0.001$, values represent mean ± SEM.

(B) RAB-soluble fractions from tau KO, PBS-treated, and the anti-tau antibody-treated mice were incubated with unconjugated protein-G-agarose beads at 4°C with end-over-end rotation for 24 hr. This precipitates any residual antibody in the brain, including antibody bound to tau seeds. Elution of any seeding activity from the antibody/bead complexes was measured by FRET assay. There was significantly less seeding activity observed in HJ8.5 and HJ9.3 antibody-treated mice versus PBS-treated mice ****$p < 0.0001$, values represent mean ± SEM.

(C) Seventy percent FA fractions of 9-month-old P301S brain cortex region of all treated groups analyzed by ELISA showed a strong correlation with FRET analysis performed with the RAB-soluble fractions.

(D) Comparison between tau levels (x axis) and seeding activity (y axis) present in RAB-soluble fractions of 9-month-old P301S brain cortex of all treated mice assessed. There was no significant correlation between these two measures.

(E) Tau species in the RAB-soluble fractions of 3-month-old knockout (KO), 3-month-old wild-type (WT), 3-month-old P301S, and 9-month-old PBS-treated P301S mice were separated on SDD-AGE, followed by western blotting. Polyclonal mouse anti-tau antibody was used for detecting tau species. High molecular weight tau species present in the RAB-soluble fraction in both 3-month-old P301S mice and larger amounts present in 9-month-old P301S mice.

target phospho-tau, two of three strongly reduced abnormal tau load both immunohistologically and biochemically, and two significantly improved memory, one to a greater extent than the other. Effects on tau pathology also correlated very well with a reduction in intrinsic seeding activity.

HJ8.5 and HJ9.3 strongly decreased pathological tau seeds in vivo. A strong reduction in tau pathology might occur by preventing induction of tau aggregation in neighboring cells. While HJ9.4 did not decrease pathology as potently, it did decrease tau pathology in the amygdala. The variation in effectiveness in different brain regions among the antibodies may be due to the formation of region-specific aggregate conformers for which the antibodies have subtle differences in binding affinity.

Once extracellular tau aggregates are sequestered by anti-tau antibodies in vivo, their metabolic fate is not yet clear. After 3 months of antibody administration, we found reduced microglial activation, presumably due to less tau-related pathology and neurodegeneration. Several months of passive immunization with anti-Aβ antibodies has also been noted to reduce microgliosis (Wilcock et al., 2003). The mechanism by which antibody/tau complexes are cleared in vivo, and the mechanism via which they decrease tau pathology, remains to be definitively clarified. It has been suggested that immunization with anti-α-synuclein antibodies clears α-synuclein aggregates by promoting lysosomal degradation (Masliah et al., 2011). A recent study with anti-α-synuclein antibodies showed that the antibodies targeted α-synuclein clearance mainly via microglia, presumably through Fc receptors (Bae et al., 2012). Neurons express Fcγ receptors (Andoh and Kuraishi, 2004; Mohamed et al., 2002) and may be able to internalize IgG complexed with antigen by high-affinity FcγRI receptor (Ravetch and Bolland, 2001). Internalized tau antibodies may contact tau in endosomes and eventually induce clearance of intracellular tau aggregates by the endosomal/lysosomal system (Sigurdsson, 2009). Though the anti-tau antibodies used in our current study can bind extracellular tau assemblies, we found no evidence of significant localization within cells. However, that does not rule out the possibility that cells in vivo take up antibody/tau

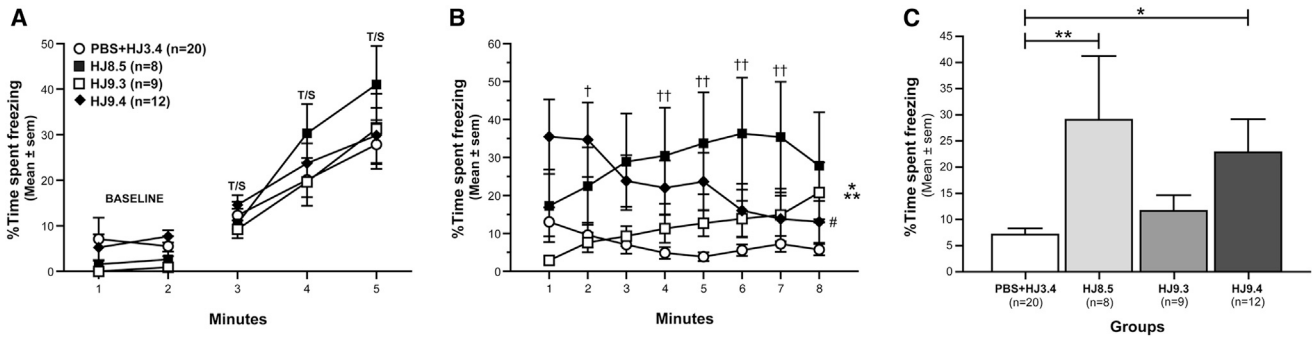

Figure 8. Contextual Fear Conditioning Deficits in P301S Tau Transgenic Mice Are Rescued by HJ8.5 and HJ9.4 Antibody Treatments

(A) On day 1 of conditioned fear testing, no differences were observed among groups in freezing levels during either the 2 min baseline condition or the tone/shock (T/S) training as indicated by the lack of a significant main or interaction effects involving treatment after repeated-measures ANOVAs on these data.

(B) In contrast, a significant effect of treatment (*p = 0.019) and a significant treatment by minutes interaction (**p = 0.0001) were observed after a repeated-measures ANOVA on freezing levels during the contextual fear testing on day 2. Only the HJ9.4 group showed significant habituation from minute 1 versus minute 8 (#p = 0.002).

(C) Subsequent planned comparisons showed that freezing in the HJ8.5 and HJ9.4 tau antibody groups was significantly increased relative to the PBS+HJ3.4 control group when averaged across the 8 min session (**p = 0.006 and *p = 0.022, respectively). However, further analyses of the data showed that the largest differences between the HJ9.4 group and the PBS+HJ3.4 controls occurred during minute 2 (†p = 0.004), while the largest differences between the HJ8.5-treated mice and the control group were found during minutes 4–7 (††p < 0.004) as depicted in (B). Values represent mean ± SEM.

complexes to influence tau aggregate clearance. For example, it has recently been shown that antibodies complexed with viruses can bind to the cytosolic IgG receptor TRIM21, targeting the antibody/virus complex to the proteasome (Mallery et al., 2010). In addition, antibodies bound to TRIM21 were shown to activate immune signaling (McEwan et al., 2013). Interestingly, there is also evidence in the P301S model of tauopathy that the innate immune system is activated prior to the development of significant tau pathology and that early immunosuppression attenuates tau pathology (Yoshiyama et al., 2007). It is possible that antibodies capture tau aggregates induced by inflammation, reducing subsequent aggregate-induced inflammation and disease progression.

Extracellular Tau and Spreading of Tau Pathology

Our work implicitly tests the role of extracellular tau in pathogenesis. It is now clear that extracellular tau aggregates can trigger fibril formation of native tau inside cells, whether their source is recombinant protein or tau extracted from mammalian cells (Clavaguera et al., 2009; de Calignon et al., 2010; Frost et al., 2009; Guo and Lee, 2011; Liu et al., 2012). We originally hypothesized a role for free tau aggregates (i.e., not membrane enclosed) as mediators of *trans*-cellular propagation based on our prior work, because HJ9.3 added to the cell media blocked internalization and immunoprecipitated free fibrils (Kfoury et al., 2012).

In animal models, tau aggregates can apparently spread from one region to another (de Calignon et al., 2012; Liu et al., 2012). We found that monomeric tau is constantly released in vivo into the brain interstitial fluid even under nonpathological conditions (Yamada et al., 2011). We also found that exogenous aggregates would reduce levels of soluble ISF tau, suggesting that seeding and/or sequestration phenomena can occur in this space (Yamada et al., 2011). Taken together, evidence supports the concept that extracellular tau aggregates form and can be taken up by adjacent cells, connected cells, or possibly back into the same cell, thereby increasing the burden of protein aggregation. This evidence makes a clear prediction: therapy that captures extracellular seeding activity should ameliorate disease.

The Role of Tau Flux in Pathogenesis

It would not be predicted a priori that a mouse model such as P301S, which drives mutant tau expression via the prion promoter in virtually all neurons, should benefit from antibody treatments that block *trans*-cellular propagation of aggregation. In theory, pathology could occur independently in all neurons that express this aggregation-prone protein. However, our prior work in tissue culture suggested a role for flux of tau aggregates (Kfoury et al., 2012). While the model of aggregate flux requires further testing, our results here are consistent with this idea, since antibody treatment profoundly reduced intracellular tau pathology. We predict that antibodies that block tau uptake will create a "sink" in the extracellular space that will promote clearance by another mechanism, possibly involving microglia.

Therapeutic Antibodies and Targeting Seeding Activity

There are increasing efforts to develop therapeutic antibodies that target aggregation-prone proteins that accumulate within cells. The principal criteria have been that the antibodies will bind epitopes known to accumulate in diseased brain. This approach may or may not lead to antibodies with optimal activity in vivo. Our work supports a model of therapeutic antibody development that emphasizes efficacy in blocking the seeding activity present in the brain, rather than specific linear epitopes. Using this approach we identified antibodies with higher apparent efficacy than has previously been reported. In an extension of the prion hypothesis, we propose further that distinct tau aggregate "strains" may predominate in patients with different types of tauopathy, and these may have unique sensitivities to different antibodies. The use of sensitive in vitro

assays of antibody efficacy may allow much more efficient development and optimization of antibody-based therapies.

The strong protective effect of the anti-tau antibodies, particularly with the HJ8.5 antibody, suggests that this type of approach should be considered as a treatment strategy for human tauopathies. In addition to our ICV approach, it will be important to determine the PK/PD response with peripheral administration of these antibodies. The tau seeding assay may be useful to monitor target engagement by the antibodies.

EXPERIMENTAL PROCEDURES

Antibodies

HJ9.3 and HJ9.4 mouse monoclonal antibodies were raised by immunizing tau knockout mice (The Jackson Laboratory) against mouse tau, and HJ8.5 and HJ8.7 monoclonal antibodies were raised by immunizing tau knockout mice against human tau. Detailed information of the different antibodies used is provided in Supplemental Information.

Animals

P301S tau transgenic mice (purchased from The Jackson Laboratory), which express the P301S human T34 isoform (1N4R), were generated and characterized previously (Yoshiyama et al., 2007). These mice are on a B6C3 background. Animal procedures were performed according to protocols approved by the Animal Studies Committee at Washington University School of Medicine.

Surface Plasmon Resonance

Surface plasmon resonance experiments were performed as described with minor modifications (Basak et al., 2012) (see Supplemental Information).

Intracerebroventricular Injection Procedure

Intracerebroventricular (ICV) infusions were performed by Alzet osmotic pumps, 2006 model (Durect). Detailed surgery procedure is provided in Supplemental Information.

Immunofluorescence

Immunofluorescence was performed as previously described (Kfoury et al., 2012) with some modifications (see Supplemental Information).

Cell Culture/Seeding Assay: P301S Brain Lysates and Antibody Treatment

Experiments were performed similar to those previously described (Kfoury et al., 2012) with some modifications (see Supplemental Information).

Immunoprecipitation

Immunoprecipitation was performed similar to previously described (Kfoury et al., 2012) with some modifications (see Supplemental Information).

Depletion and Immunoprecipitation of Tau Aggregates from P301S Brain Using Tau-Specific Antibodies

Immunoprecipitation of tau and tau aggregates was performed as described (Kfoury et al., 2012) with some modifications (see Supplemental Information).

Atomic Force Microscope

Atomic force microscopy was performed as previously described (Kfoury et al., 2012) with some modifications (see Supplemental Information).

Histology

After 12 weeks of the treatment, P301S mice were anesthetized with intraperitoneal pentobarbital (200 mg/kg) followed by perfusion with 3 U/ml heparin in cold Dulbecco's PBS. Detailed procedure is provided in Supplemental Information.

Immunohistochemistry

Immunohistochemistry was performed as described previously (DeMattos et al., 2001) with minor modifications (see Supplemental Information).

Brain Tissue Extraction

Brain tissue extractions were performed as described previously (Yamada et al., 2011) with minor modifications (see Supplemental Information).

Interperitoneal Injection and ICV Administration of Biotinylated HJ8.5 Antibody

Mouse monoclonal HJ8.5 antibody was biotinylated according to the manufacturer's instructions (Sulfo-NHS-LC-Biotin kit, Pierce). Detailed procedure is provided in Supplemental Information.

ELISA to Detect Free HJ8.5B and HJ8.5B Bound to Tau

The concentration of free HJ8.5B was determined in serum and CSF of mice 48 hr after IP or ICV administration. Detailed procedure is provided in Supplemental Information.

Semidenaturing Detergent-Agarose Gel Electrophoresis

SDD-AGE was performed as described previously (Kryndushkin et al., 2003) with minor modifications (see Supplemental Information).

Electrophoresis and Immunoblotting

These experiments were performed as described previously (Yamada et al., 2011) with minor modifications (see Supplemental Information).

Tau Sandwich ELISA Assays

ELISAs were performed as described previously (Yamada et al., 2011) with minor modifications (see Supplemental Experimental Procedures).

Statistical Analysis Applying Treatment and Gender as Factors

The control group (PBS and HJ3.4) mean was compared with each treatment group mean. Detailed procedures are provided in Supplemental Information.

Behavioral Tests

Tests were performed as described previously (Ghoshal et al., 2012; Sato et al., 2012; Wozniak et al., 2007) with minor modifications (see Supplemental Information).

Statistical Analyses of Behavioral Data

ANOVA models were typically used to analyze the behavioral data (Systat 12, Systat Software). Detailed procedures are provided in Supplemental Information.

Statistical Analysis of Pathological and Biochemical Data

All data are presented as mean ± SEM, and different conditions were compared using one-way ANOVA followed by Dunnett's post hoc test to compare controls with treatment groups. Statistical significance was set at $p < 0.05$. Statistics were performed using GraphPad Prism 5.04 for Windows (GraphPad Software). For quantitative assessment of AT8 staining, gender is a significant factor, so results were adjusted by gender using SAS version 9.2 software.

SUPPLEMENTAL INFORMATION

Supplemental Information includes Supplemental Experimental Procedures and eight figures and can be found with this article online at http://dx.doi.org/10.1016/j.neuron.2013.07.046.

ACKNOWLEDGMENTS

Funding for this study was from the Tau consortium (D.M.H. and M.I.D.) and from a research grant from C2N Diagnostics (D.M.H. and M.I.D.). D.M.H. is a cofounder and has ownership interests in C2N Diagnostics. We thank Floy Stewart and Mary Beth Finn for expert technical advice and assistance.

Accepted: July 29, 2013
Published: September 26, 2013

REFERENCES

Andoh, T., and Kuraishi, Y. (2004). Direct action of immunoglobulin G on primary sensory neurons through Fc gamma receptor I. FASEB J. *18*, 182–184.

Arriagada, P.V., Growdon, J.H., Hedley-Whyte, E.T., and Hyman, B.T. (1992). Neurofibrillary tangles but not senile plaques parallel duration and severity of Alzheimer's disease. Neurology *42*, 631–639.

Asuni, A.A., Boutajangout, A., Quartermain, D., and Sigurdsson, E.M. (2007). Immunotherapy targeting pathological tau conformers in a tangle mouse model reduces brain pathology with associated functional improvements. J. Neurosci. *27*, 9115–9129.

Bae, E.J., Lee, H.J., Rockenstein, E., Ho, D.H., Park, E.B., Yang, N.Y., Desplats, P., Masliah, E., and Lee, S.J. (2012). Antibody-aided clearance of extracellular α-synuclein prevents cell-to-cell aggregate transmission. J. Neurosci. *32*, 13454–13469.

Bancher, C., Braak, H., Fischer, P., and Jellinger, K.A. (1993). Neuropathological staging of Alzheimer lesions and intellectual status in Alzheimer's and Parkinson's disease patients. Neurosci. Lett. *162*, 179–182.

Bard, F., Cannon, C., Barbour, R., Burke, R.L., Games, D., Grajeda, H., Guido, T., Hu, K., Huang, J., Johnson-Wood, K., et al. (2000). Peripherally administered antibodies against amyloid beta-peptide enter the central nervous system and reduce pathology in a mouse model of Alzheimer disease. Nat. Med. *6*, 916–919.

Basak, J.M., Verghese, P.B., Yoon, H., Kim, J., and Holtzman, D.M. (2012). Low-density lipoprotein receptor represents an apolipoprotein E-independent pathway of Aβ uptake and degradation by astrocytes. J. Biol. Chem. *287*, 13959–13971.

Bi, M., Ittner, A., Ke, Y.D., Götz, J., and Ittner, L.M. (2011). Tau-targeted immunization impedes progression of neurofibrillary histopathology in aged P301L tau transgenic mice. PLoS ONE *6*, e26860.

Boimel, M., Grigoriadis, N., Lourbopoulos, A., Haber, E., Abramsky, O., and Rosenmann, H. (2010). Efficacy and safety of immunization with phosphorylated tau against neurofibrillary tangles in mice. Exp. Neurol. *224*, 472–485.

Boutajangout, A., Quartermain, D., and Sigurdsson, E.M. (2010). Immunotherapy targeting pathological tau prevents cognitive decline in a new tangle mouse model. J. Neurosci. *30*, 16559–16566.

Boutajangout, A., Ingadottir, J., Davies, P., and Sigurdsson, E.M. (2011). Passive immunization targeting pathological phospho-tau protein in a mouse model reduces functional decline and clears tau aggregates from the brain. J. Neurochem. *118*, 658–667.

Braak, H., and Braak, E. (1997). Diagnostic criteria for neuropathologic assessment of Alzheimer's disease. Neurobiol. Aging Suppl. *18*, S85–S88.

Chai, X., Wu, S., Murray, T.K., Kinley, R., Cella, C.V., Sims, H., Buckner, N., Hanmer, J., Davies, P., O'Neill, M.J., et al. (2011). Passive immunization with anti-Tau antibodies in two transgenic models: reduction of Tau pathology and delay of disease progression. J. Biol. Chem. *286*, 34457–34467.

Clavaguera, F., Bolmont, T., Crowther, R.A., Abramowski, D., Frank, S., Probst, A., Fraser, G., Stalder, A.K., Beibel, M., Staufenbiel, M., et al. (2009). Transmission and spreading of tauopathy in transgenic mouse brain. Nat. Cell Biol. *11*, 909–913.

de Calignon, A., Fox, L.M., Pitstick, R., Carlson, G.A., Bacskai, B.J., Spires-Jones, T.L., and Hyman, B.T. (2010). Caspase activation precedes and leads to tangles. Nature *464*, 1201–1204.

de Calignon, A., Polydoro, M., Suárez-Calvet, M., William, C., Adamowicz, D.H., Kopeikina, K.J., Pitstick, R., Sahara, N., Ashe, K.H., Carlson, G.A., et al. (2012). Propagation of tau pathology in a model of early Alzheimer's disease. Neuron *73*, 685–697.

DeMattos, R.B., Bales, K.R., Cummins, D.J., Dodart, J.C., Paul, S.M., and Holtzman, D.M. (2001). Peripheral anti-A beta antibody alters CNS and plasma A beta clearance and decreases brain A beta burden in a mouse model of Alzheimer's disease. Proc. Natl. Acad. Sci. USA *98*, 8850–8855.

Dodart, J.C., Bales, K.R., Gannon, K.S., Greene, S.J., DeMattos, R.B., Mathis, C., DeLong, C.A., Wu, S., Wu, X., Holtzman, D.M., and Paul, S.M. (2002). Immunization reverses memory deficits without reducing brain Abeta burden in Alzheimer's disease model. Nat. Neurosci. *5*, 452–457.

Drechsel, D.N., Hyman, A.A., Cobb, M.H., and Kirschner, M.W. (1992). Modulation of the dynamic instability of tubulin assembly by the microtubule-associated protein tau. Mol. Biol. Cell *3*, 1141–1154.

Frost, B., and Diamond, M.I. (2010). Prion-like mechanisms in neurodegenerative diseases. Nat. Rev. Neurosci. *11*, 155–159.

Frost, B., Jacks, R.L., and Diamond, M.I. (2009). Propagation of tau misfolding from the outside to the inside of a cell. J. Biol. Chem. *284*, 12845–12852.

Ghoshal, N., Dearborn, J.T., Wozniak, D.F., and Cairns, N.J. (2012). Core features of frontotemporal dementia recapitulated in progranulin knockout mice. Neurobiol. Dis. *45*, 395–408.

Goedert, M., Jakes, R., and Vanmechelen, E. (1995). Monoclonal antibody AT8 recognises tau protein phosphorylated at both serine 202 and threonine 205. Neurosci. Lett. *189*, 167–169.

Guo, J.L., and Lee, V.M. (2011). Seeding of normal Tau by pathological Tau conformers drives pathogenesis of Alzheimer-like tangles. J. Biol. Chem. *286*, 15317–15331.

Halfmann, R., and Lindquist, S. (2008). Screening for amyloid aggregation by semi-denaturing detergent-agarose gel electrophoresis. J. Vis. Exp. Published online July 16, 2008. http://dx.doi.org/10.3791/838.

Iba, M., Guo, J.L., McBride, J.D., Zhang, B., Trojanowski, J.Q., and Lee, V.M. (2013). Synthetic tau fibrils mediate transmission of neurofibrillary tangles in a transgenic mouse model of Alzheimer's-like tauopathy. J. Neurosci. *33*, 1024–1037.

Jeganathan, S., von Bergen, M., Mandelkow, E.M., and Mandelkow, E. (2008). The natively unfolded character of tau and its aggregation to Alzheimer-like paired helical filaments. Biochemistry *47*, 10526–10539.

Jicha, G.A., Weaver, C., Lane, E., Vianna, C., Kress, Y., Rockwood, J., and Davies, P. (1999). cAMP-dependent protein kinase phosphorylations on tau in Alzheimer's disease. J. Neurosci. *19*, 7486–7494.

Kfoury, N., Holmes, B.B., Jiang, H., Holtzman, D.M., and Diamond, M.I. (2012). Trans-cellular propagation of Tau aggregation by fibrillar species. J. Biol. Chem. *287*, 19440–19451.

Kim, W., Lee, S., Jung, C., Ahmed, A., Lee, G., and Hall, G.F. (2010). Interneuronal transfer of human tau between Lamprey central neurons in situ. J. Alzheimers Dis. *19*, 647–664.

Kotilinek, L.A., Bacskai, B., Westerman, M., Kawarabayashi, T., Younkin, L., Hyman, B.T., Younkin, S., and Ashe, K.H. (2002). Reversible memory loss in a mouse transgenic model of Alzheimer's disease. J. Neurosci. *22*, 6331–6335.

Kryndushkin, D.S., Alexandrov, I.M., Ter-Avanesyan, M.D., and Kushnirov, V.V. (2003). Yeast [PSI+] prion aggregates are formed by small Sup35 polymers fragmented by Hsp104. J. Biol. Chem. *278*, 49636–49643.

Liu, L., Drouet, V., Wu, J.W., Witter, M.P., Small, S.A., Clelland, C., and Duff, K. (2012). Trans-synaptic spread of tau pathology in vivo. PLoS ONE *7*, e31302.

Macauley, S.L., Pekny, M., and Sands, M.S. (2011). The role of attenuated astrocyte activation in infantile neuronal ceroid lipofuscinosis. J. Neurosci. *31*, 15575–15585.

Mallery, D.L., McEwan, W.A., Bidgood, S.R., Towers, G.J., Johnson, C.M., and James, L.C. (2010). Antibodies mediate intracellular immunity through tripartite motif-containing 21 (TRIM21). Proc. Natl. Acad. Sci. USA *107*, 19985–19990.

Mandelkow, E.M., and Mandelkow, E. (2012). Biochemistry and cell biology of tau protein in neurofibrillary degeneration. Cold Spring Harb Perspect Med *2*, a006247.

Masliah, E., Rockenstein, E., Mante, M., Crews, L., Spencer, B., Adame, A., Patrick, C., Trejo, M., Ubhi, K., Rohn, T.T., et al. (2011). Passive immunization reduces behavioral and neuropathological deficits in an alpha-synuclein transgenic model of Lewy body disease. PLoS ONE *6*, e19338.

McEwan, W.A., Tam, J.C., Watkinson, R.E., Bidgood, S.R., Mallery, D.L., and James, L.C. (2013). Intracellular antibody-bound pathogens stimulate immune signaling via the Fc receptor TRIM21. Nat. Immunol. *14*, 327–336.

Mohamed, H.A., Mosier, D.R., Zou, L.L., Siklós, L., Alexianu, M.E., Engelhardt, J.I., Beers, D.R., Le, W.D., and Appel, S.H. (2002). Immunoglobulin Fc gamma receptor promotes immunoglobulin uptake, immunoglobulin-mediated calcium increase, and neurotransmitter release in motor neurons. J. Neurosci. Res. *69*, 110–116.

Otvos, L., Jr., Feiner, L., Lang, E., Szendrei, G.I., Goedert, M., and Lee, V.M. (1994). Monoclonal antibody PHF-1 recognizes tau protein phosphorylated at serine residues 396 and 404. J. Neurosci. Res. *39*, 669–673.

Polydoro, M., Acker, C.M., Duff, K., Castillo, P.E., and Davies, P. (2009). Age-dependent impairment of cognitive and synaptic function in the htau mouse model of tau pathology. J. Neurosci. *29*, 10741–10749.

Raj, A., Kuceyeski, A., and Weiner, M. (2012). A network diffusion model of disease progression in dementia. Neuron *73*, 1204–1215.

Ravetch, J.V., and Bolland, S. (2001). IgG Fc receptors. Annu. Rev. Immunol. *19*, 275–290.

Rosenmann, H., Grigoriadis, N., Karussis, D., Boimel, M., Touloumi, O., Ovadia, H., and Abramsky, O. (2006). Tauopathy-like abnormalities and neurologic deficits in mice immunized with neuronal tau protein. Arch. Neurol. *63*, 1459–1467.

Santa-Maria, I., Varghese, M., Ksiezak-Reding, H., Dzhun, A., Wang, J., and Pasinetti, G.M. (2012). Paired helical filaments from Alzheimer disease brain induce intracellular accumulation of Tau protein in aggresomes. J. Biol. Chem. *287*, 20522–20533.

Sato, C., Turkoz, M., Dearborn, J.T., Wozniak, D.F., Kopan, R., and Hass, M.R. (2012). Loss of RBPj in postnatal excitatory neurons does not cause neurodegeneration or memory impairments in aged mice. PLoS ONE *7*, e48180.

Seeley, W.W., Crawford, R.K., Zhou, J., Miller, B.L., and Greicius, M.D. (2009). Neurodegenerative diseases target large-scale human brain networks. Neuron *62*, 42–52.

Sigurdsson, E.M. (2009). Tau-focused immunotherapy for Alzheimer's disease and related tauopathies. Curr. Alzheimer Res. *6*, 446–450.

Small, S.A., and Duff, K. (2008). Linking Abeta and tau in late-onset Alzheimer's disease: a dual pathway hypothesis. Neuron *60*, 534–542.

Strazielle, N., and Ghersi-Egea, J.F. (2013). Physiology of blood-brain interfaces in relation to brain disposition of small compounds and macromolecules. Mol. Pharm. *10*, 1473–1491.

Troquier, L., Caillierez, R., Burnouf, S., Fernandez-Gomez, F.J., Grosjean, M.E., Zommer, N., Sergeant, N., Schraen-Maschke, S., Blum, D., and Buee, L. (2012). Targeting phospho-Ser422 by active Tau Immunotherapy in the THYTau22 mouse model: a suitable therapeutic approach. Curr. Alzheimer Res. *9*, 397–405.

Wilcock, D.M., DiCarlo, G., Henderson, D., Jackson, J., Clarke, K., Ugen, K.E., Gordon, M.N., and Morgan, D. (2003). Intracranially administered anti-Abeta antibodies reduce beta-amyloid deposition by mechanisms both independent of and associated with microglial activation. J. Neurosci. *23*, 3745–3751.

Witman, G.B., Cleveland, D.W., Weingarten, M.D., and Kirschner, M.W. (1976). Tubulin requires tau for growth onto microtubule initiating sites. Proc. Natl. Acad. Sci. USA *73*, 4070–4074.

Wozniak, D.F., Xiao, M., Xu, L., Yamada, K.A., and Ornitz, D.M. (2007). Impaired spatial learning and defective theta burst induced LTP in mice lacking fibroblast growth factor 14. Neurobiol. Dis. *26*, 14–26.

Yamada, K., Cirrito, J.R., Stewart, F.R., Jiang, H., Finn, M.B., Holmes, B.B., Binder, L.I., Mandelkow, E.M., Diamond, M.I., Lee, V.M., and Holtzman, D.M. (2011). In vivo microdialysis reveals age-dependent decrease of brain interstitial fluid tau levels in P301S human tau transgenic mice. J. Neurosci. *31*, 13110–13117.

Yoshiyama, Y., Higuchi, M., Zhang, B., Huang, S.M., Iwata, N., Saido, T.C., Maeda, J., Suhara, T., Trojanowski, J.Q., and Lee, V.M. (2007). Synapse loss and microglial activation precede tangles in a P301S tauopathy mouse model. Neuron *53*, 337–351.

Zhang, B., Carroll, J., Trojanowski, J.Q., Yao, Y., Iba, M., Potuzak, J.S., Hogan, A.M., Xie, S.X., Ballatore, C., Smith, A.B., 3rd., et al. (2012). The microtubule-stabilizing agent, epothilone D, reduces axonal dysfunction, neurotoxicity, cognitive deficits, and Alzheimer-like pathology in an interventional study with aged tau transgenic mice. J. Neurosci. *32*, 3601–3611.

Zhou, J., Gennatas, E.D., Kramer, J.H., Miller, B.L., and Seeley, W.W. (2012). Predicting regional neurodegeneration from the healthy brain functional connectome. Neuron *73*, 1216–1227.